Non-aggregating zinc phthalocyanine sensitizer with bulky diphenylphenoxy donor groups and pyrazole-3-carboxylic acid anchoring group for coadsorbent-free dye-sensitized solar cells

Burak Yıldız [a], Barış Seçkin Arslan [b], Emre Güzel [c], Mehmet Nebioğlu [b,d,e], Nurettin Menges [f], İlkay Şişman [b,d,e,*], M. Kasım Şener [a,*]

[a] Department of Chemistry, Yıldız Technical University, 34210 İstanbul, Turkey
[b] Department of Chemistry, Sakarya University, 54050 Sakarya, Turkey
[c] Department of Fundamental Sciences, Sakarya University of Applied Sciences, Sakarya, Turkey
[d] Department of Renewable Energy Systems, Sakarya University, Sakarya, Turkey
[e] Biomedical, Magnetic and Semiconductor Materials Research Center (BIMAS-RC), Sakarya University, Sakarya, Turkey
[f] Department of Pharmaceutical Chemistry, Yüzüncü Yıl University, 65090 Van, Turkey

ARTICLE INFO

ABSTRACT

A novel unsymmetrical zinc phthalocyanine complex (**PCA-ZnPc-3**) containing six 2,6-diphenylphenoxy donor groups and pyrazole-3-carboxylic acid anchoring group has been synthesized and used as a sensitizer for dye-sensitized solar cells (DSSCs). The optical, electrochemical and photovoltaic characteristics were evaluated and compared with the dyes containing the same anchoring group and *tert*-butyl (**PCA-ZnPc-1**) or hexylsulfanyl (**PCA-ZnPc-2**) donor groups, developed by our group. The DSSC with **PCA-ZnPc-3** exhibited a higher power conversion efficiency (PCE) of 2.04% as compared to that of **PCA-ZnPc-1** (PCE = 1.74%) and **PCA-ZnPc-2** (PCE = 1.89%). This enhancement in efficiency may be ascribed to the less dye aggregation and appropriate dye coverage. These results suggest that the incorporation of 2,6-diphenylphenoxy into pyrazole-3-carboxylic acid-based zinc phthalocyanine sensitizers can improve photovoltaic performance of DSSCs.

1. Introduction

One of the most important scientific and technological research topics of this century is to replace fossil fuels with renewable energy sources. Among this energy sources, solar energy has an important place in terms of sustainability. Since the report by Gratzel in 1991, DSSCs utilizing nanoporous TiO_2 electrode have been attracted much attention because of their low cost in comparison with silicon-based photovoltaic devices (Matsuzaki et al., 2014). Polypyridyl-ruthenium complexes (**N3, N719**) with a PCE of up to 12% are the most successful dyes in this field (Yu et al., 2012). However, ruthenium-based dyes have disadvantages such as lack of absorption in the red/near-infrared region, their high cost, and the rarity of the metal (Shi et al., 2015). To produce highly efficient DSSCs, sensitizers are required to absorb red/near-infrared region of solar spectrum (Matsuzaki et al., 2014).

Phthalocyanines are very convenient sensitizers for DSSCs because of

their light absorption in the UV and red/near-infrared region, high extinction coefficients, photochemical and thermal stability (Cid et al., 2009; Ragoussi et al., 2012). Therefore, many symmetric phthalocyanines have been used or tested as sensitizers in DSSC but they have showed low PCEs due to dyes' aggregation and solubility problem in organic solvents. In order to prevent such problems, unsymmetrical phthalocyanines bearing bulky aliphatic or aromatic donor groups and "anchoring group", i.e., a chemical substituent able to adsorb the dye molecule onto the TiO_2 surface, have been used in DSSCs (Yıldız et al., 2019). At short intervals in 2007, two unsymmetrical zinc phthalocyanines, **PCH001** and **TT1**, having three *tert*-butyl donor groups and different anchoring group (succinic acid for **PCH001**, carboxylic acid for **TT1**), were reported (Cid et al., 2007; Reddy et al., 2007). With **PCH001** and **TT1**, the highest power conversion efficiencies were obtained in phthalocyanine-sensitized solar cells for that time (**PCH001** 3.05%, **TT1** 3.52%). After this reports, a large number of ABBB type unsymmetrical

Scheme 1. Synthesis of **PCA-ZnPc-3**. (i) ZnCl$_2$, DBU, n-pentanol, 72 h; (ii) 1 M NaOH, THF, 60 °C, 48 h.

zinc phthalocyanine dyes with different bulky donor groups and anchoring group have been tested for DSSCs. Although unsymmetrical zinc phthalocyanines have less tendency to aggregation as compared to their symmetric derivatives, coadsorbent have been still used to prevent dye aggregation on TiO$_2$ surface (Mori et al., 2010). However, the necessary amount of coadsorbent per dye molecule to reach the optimal efficiency is usally huge, which constitutes a major drawback because it reduces the total number of adsorbed dye molecules on the surface thus the absolute amount of injected electrons from the excited-dye to the electrode, which in fine limits the current density of the cell (Urbani et al., 2019). In 2010, Mori et al. reported a new unsymmetrical zinc phthalocyanine containing 2,6-diphenylphenoxy groups (**PcS6**), succeeding in completely prevent to aggregation without using a coadsorbent (Ragoussi et al., 2013). They had achieved high power conversion efficiency (4.60%) using **PcS6** for DSSCs. This unsymmetrical phthalocyanine derivative had been a new breakthrough for phthalocyanine-sensitized solar cells, and many phthalocyanine derivatives bearing 2,6-diphenylphenoxy groups have been synthesized and used for DSSCs. Phthalocyanine derivative containing 2,6-diphenylphenoxy donor groups reported by Ragoussi et al in 2012, has highest power conversion efficiency among DSSCs using phthalocyanine dyes.

A short time ago, we have reported phthalocyanine dyes, **PCA-ZnPc-1** and **PCA-ZnPc-2**, having three *tert*-butyl and six hexylsulfanyl donor groups, respectively, and pyrazole-3-carboxylic acid anchoring group. Pyrazole-3-carboxylic acid has two N-donors on the pyrazole ring and two O-donors on the carboxylate and this N and O atoms can chelate very stable with metal ions (Saçmacı and Kartal, 2008; Şener et al., 2004). Thus, electron injection efficiency of the dye and stability of the cell can be increased using pyrazole-3-carboxylic acid anchoring group in phthalocyanine-sensitized solar cells. It has been seen that **PCA-ZnPc-1** had 2.5 times higher power conversion efficiency with respect to **TT4** bearing *tert*-butyl donor groups and carboxylic acid anchoring group. However, utilizing chenodeoxycholic acid (CDCA) as coadsorbent was

necessary to reach maximum PCE for **PCA-ZnPc-1** and **PCA-ZnPc-2** sensitized solar cells. In this study, to eliminate the above-mentioned problems caused by the use of coadsorbent CDCA, we have synthesized new unsymmetrical zinc phthalocyanine, **PCA-ZnPc-3**, having six bulky diphenylphenoxy donor groups and pyrazole-3-carboxylic acid anchoring group and used as a sensitizer for DSSCs.

2. Experimental

2.1. Synthesis of 4-(4-(3-(ethoxycarbonyl)-1H-pyrazole-5-yl)phenoxy) phthalonitrile 1

4-Nitrophthalonitrile (100 mg, 0.578 mmol) and 5-(4-hydroxyphenyl)-2H-pyrazole-3-carboxylic acid ethyl ester (201 mg, 0.867 mmol) were dissolved in 20 mL dry DMF. Anhydrous potassium carbonate (106 mg, 0.77 mmol) was added to the reaction solution in portionwise over 2 h. The reaction mixture was stirred vigorously at room temperature during 3 days under argon atmosphere. The mixture was poured into ice-water (300 mL). The white precipitate was collected by filtration, dried under vacuum and recrystallized from ethanol (Yıldız et al., 2018). Yield 170 mg (82.1%), M.p: 230 °C.

2.2. Synthesis of 4,5-bis(2,6-diphenylphenoxy)phthalonitrile 2

4,5-Dichlorophthalonitrile (200 mg; 1.015 mmol), 2,6-diphenylphenol (750 mg; 3.045 mmol) were dissolved in 5 mL anhydrous DMF and dry K$_2$CO$_3$ (1.4 g; 10.15 mmol) was added. Reaction mixture was mixed at 100 °C for 36 h. The mixture was cooled to room temperature and poured into ice-water. Then mixture was extracted with dichloromethane DCM (3 × 50 mL). Organic phase was dried over Na$_2$SO$_4$ and evaporated. The residue was purified by column chromatography using DCM as the eluent. Recrystallization from methanol gave white solid (Mori et al., 2010). Yield: 286 mg (46%). ATR-IR (υ, cm^{-1}): 3072–3035

(CH, aromatic), 2229 (C≡N). ^{1}H NMR (CDCl₃), (δ, ppm): 7.46 (6H), 7.42 (8H), 7.15 (4H), 7.06 (8H), 6.25 (2H).

2.3. Synthesis of 2,3,9,10,16,17-hexa(2,6-diphenylphenoxy)-23-mono (4-(3-(ethoxycarbonyl)-1H-pyrazole-5-yl)phenoxy)phthalocyaninatozinc (II) 3

1 (45.8 mg, 0.128 mmol), **2** (236.4 mg, 0.384 mmol) were heated at reflux in n-pentanol (5 mL) under argon atmosphere for 72 h in the presence of ZnCl₂ (23.3 mg, 0.1705 mmol) and DBU (5 drops). After cooling to room temperature, reaction mixture was poured into methanol and resulting green precipitate was filtered off and washed with methanol. Afterwards, the green solid was purified by column chromatography on silica gel. Symmetric phthalocyanine with 2,6-diphenlphenoxy group was eluted first using DCM, and then **3** was eluted using DCM:ethanol (100:1). Yield: 30.6 mg (10.3%). ATR-IR (υ, cm^{-1}): 3055 (CH, aromatic), 2927 (CH, aliphatic), 1721 (H₁₁C₅O—C=O). MS (MALDI-TOF): m/z 2316.533 [M]$^+$. ^{1}H NMR (CDCl₃), (δ, ppm): 7.81–6.35 (Ar-H, 92H), 4.33 (2H), 3.34–3.10 (6H), 1.68 (3H). ^{13}C NMR (CDCl₃), (δ, ppm): 161.67, 148.70, 138.42, 138.29, 138.21, 137.58, 135.97, 135.91, 135.61, 135.08, 131.16, 131.10, 129.65, 129.58, 129.50, 129.27, 128.18, 127.89, 127.49, 127.32, 127.12, 127.04, 125.78, 107.80, 65.56, 38.02, 31.33, 22.27, 13.93. UV–vis (THF, 1 × 10^{-5} M) λ_{max}, nm (log ε): 681 (5.38), 614 (4.61), 358 (4.97).

2.4. Synthesis of 2,3,9,10,16,17-hexa(2,6-diphenylphenoxy)-23-mono (4-(3-(hydroxycarbonyl)-1H-pyrazole-5-yl)phenoxy)phthalocyaninato-zinc(II) PCA-ZnPc-3

1 M NaOH (0.8 mL) was added to solution of **3** (30.6 mg; 0.013 mmol) in THF. The solution was mixed at 60 °C for 48 h. Then rection mixture was cooled to room temperature and evaporated to small volume (approx. 1–2 mL). Afterwards, the precipitate acidified to pH: 1–2 with diluted HCl and water was added. The green solids were collected by centifiguration, washed with water until neutralization and dried under vacuum. Yield: 12 mg (40.4%). ATR-IR (υ, cm^{-1}): 3055 (CH, aromatic), 1715 (HO—C=O). MS (MALDI-TOF): m/z 2246.177 [M]$^+$. ^{1}H NMR (CDCl₃), (δ, ppm): 7.81–6.35 (Ar-H, 92H). ^{13}C NMR (CDCl₃), (δ, ppm): 166.07, 151.67, 145.41, 137.30, 136.94, 135.86, 135.08, 135.01, 134.01, 131.30, 131.24, 131.12, 129.34, 129.28, 128.33, 128.27, 128.19, 128.13, 128.11, 127.93, 127.69, 127.49, 125.51, 110.36. UV–vis (THF, 1 × 10^{-5} M) λ_{max}, nm (log ε): 682 (5.36), 614 (4.59), 358 (4.94).

3. Results and discussion

3.1. Synthesis and structural characterizations

In this study, firstly phthalonitrile derivatives **1** and **2** were synthesized according to the procedures described in the literature (Mori et al., 2010; Yıldız et al., 2018). Then compound **3** was obtained by mixed cyclotetramerization method from **1** and **2** in the presence of ZnCl₂ and DBU in pentanol at reflux temperature for 72 h. Under this reactions conditions, a transesterification was occured and pentyl ester form of the **3** was observed. Lastly, targeted molecule **PCA-ZnPc-3** was syhthesized by hydrolysis of the **3** (Scheme 1).

All of the new compounds were fully characterized with spectroscopic techniques such as ATR-IR, MALDI-TOF MS, ^{1}H NMR, ^{13}C NMR and UV–vis. In the ATR-IR spectrum of **3**, disappearence of the C≡N streching vibration and presence of the C=O stretching vibration at 1721 cm^{-1} support the structure. For **PCA-ZnPc-3** that synthesized by hydrolysis of **3**, C=O stretching vibration has shifted from 1721 cm^{-1} to 1715 cm^{-1} in the ATR-IR spectrum. In the MALDI-TOF MS spectra just molecular ion peaks were observed. Molecular ion peak of the **3** is at 2316.533. This result proves that transesterification has occured during the synthesis of the **3**. Molecular ion peak of the **PCA-ZnPc-3** is at
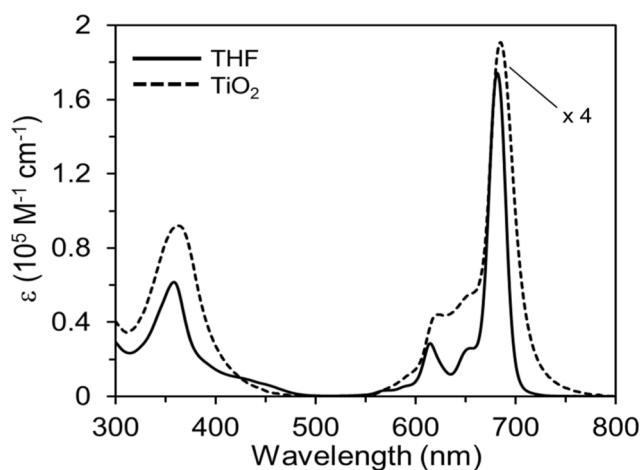

Fig. 1. Absorption spectra of **PCA-ZnPc-3** in THF (1 × 10^{-5} M) and on TiO₂ film.

2246.177 amu (Fig. S1 and S2). When ^{1}H NMR and ^{13}C NMR spectra of the new compounds were examined, aromatic peaks were observed almost the same region. Peaks belonging to ester group were observed for compound **3** at 4.33, 3.34–3.10, 1.68 ppm in ^{1}H NMR spectrum and at 65.56, 38.02, 31.33, 22.27, 13.93 ppm in ^{13}C NMR spectrum. These peaks disappeared in the spectrum of the **PCA-ZnPc-3** as expected. Additionally, in the ^{13}C NMR spectra of the **3** and **PCA-ZnPc-3**; peaks belonging to pyrazole ring for **3** at 107.80 ppm and for **PCA-ZnPc-3** at 110.36 ppm were observed.

Metallophthalocyanines have two characteristic bands in electronic absorption spectrum. One is called the Q band in the visible region at 600–800 nm, The other band is called Soret or B band between 300 and 400 nm in UV region. The reason for these two bands, π-π* transitions due to the 18 π-conjugated electrons (Sánchez-Vergara et al., 2021). UV–vis absorption spectra of the **3** and **PCA-ZnPc-3** were recorded in THF. **3** and **PCA-ZnPc-3** have same Soret band values at 358 nm. Q band values of **3** and **PCA-ZnPc-3** are at 681 nm and 682 nm, respectively. Obtained all spectral results are compatible with defined structures.

3.2. Photophysical and electrochemical characteristics

The UV–vis spectrum of **PCA-ZnPc-3** bearing 2,6-diphenylphenoxy donor groups in tetrahydrofuran (THF) shows that it contains a Soret-band at 358 nm and a Q-band at 682 nm due to π-π* ligand transition (Fig. 1). The Q-band of **PCA-ZnPc-3** is red-shifted in comparison with **PCA-ZnPc-1** based on the *tert*-butyl donors (Yıldız et al., 2018), whereas this band is blue-shifted with respect to **PCA-ZnPc-2** based on the hexylsulfanyl donors (Yıldız et al., 2019). Considering the three dyes have the same anchoring group (pyrazole-3-carboxylic acid), this result can be explained by the electron-donating ability of the 2,6-diphenylphenoxy group is between the *tert*-butyl group and the hexylsulfanyl group. The absorption spectrum of the solid dye on TiO₂ exhibits slightly broadened and red-shifted by only 3 nm relative to that in solution, indicating low aggregation on the TiO2 (Matsuzaki et al., 2014). This can be attributed to the bulky 2,6-diphenylphenoxy moieties incorporated to the dye.

Cyclic voltammogram was measured to reveal the redox behaviors of **PCA-ZnPc-3** (Fig. S3 and Table 1) (Dinçer et al., 2008). The oxidation potential (O₁) of the dye corresponding to the HOMO level is 1.20 V vs. NHE, which is lower than the potential of iodide/triiodide electrolyte (0.4 V vs. NHE), guaranteeing the dye regeneration (Jia et al., 2016). Comparing these three dyes, the HOMO level of **PCA-ZnPc-3** is between the HOMO levels of **PCA-ZnPc-1** and **PCA-ZnPc-2**. In other words, the electron-donating ability of the 2,6-diphenylphenoxy group is better than the *tert*-butyl group and worse than the hexylsulfanyl group. The

Table 1
Photophysical and electrochemical properties of **PCA-ZnPc-3**.

Dye	λ_{max} [nm] (ε [$\times 10^5$ M^{-1} cm^{-1}])	λ_{onset} [nm]	λ_{max}(TiO$_2$)[nm]	E_{0-0} [eV][a]	HOMO [V][b]	LUMO [V][c]
PCA-ZnPc-3	358 (0.62), 682 (1.74)	702	685	1.77	1.20	−0.57

[a] E_{0-0}: band gap, estimated using the formula $E_{0-0} = 1240/\lambda_{onset}$.
[b] HOMO (vs. NHE) was taken from the oxidation potential of the dye solution in DMSO.
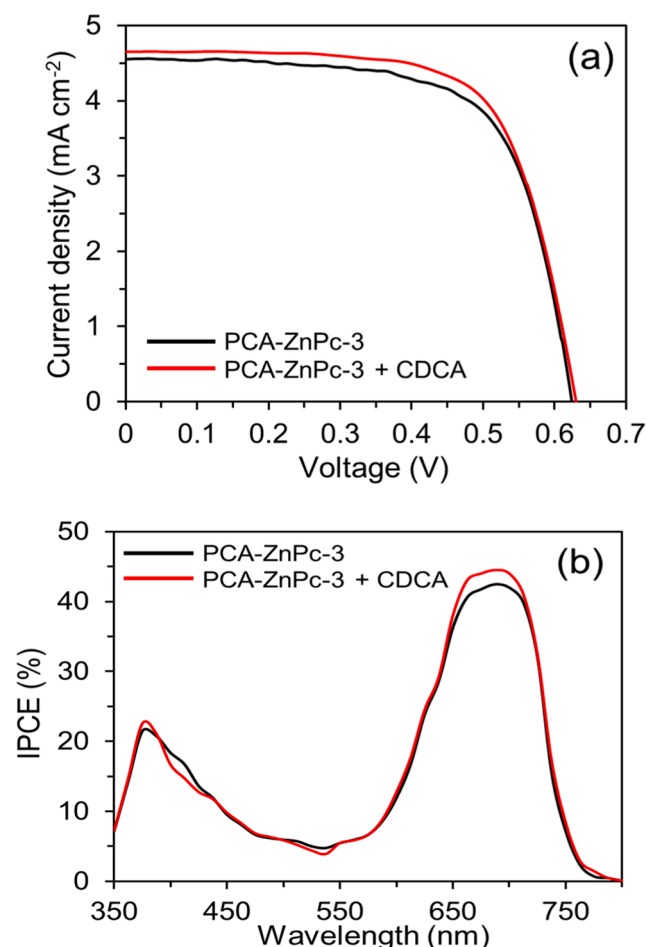[c] LUMO (vs. NHE) was obtained by HOMO − E_{0-0}.

Fig. 2. (a) *J-V* curves and (b) IPCE spectra of the DSSCs with and without CDCA.

Table 2
Photovoltaic parameters of the DSSCs.

Dye	J_{sc}^{IPCE} (mA cm^{-2})[a]	J_{sc} (mA cm^{-2})	V_{oc} (V)	FF	PCE (%)	Dye loading amount (mol cm^{-2})
PCA-ZnPc-3	4.45	4.64	0.624	0.68	1.97	3.35×10^{-8}
PCA-ZnPc-3 + CDCA	4.59	4.70	0.630	0.69	2.04	3.12×10^{-8}
TT1 + CDCA	–	7.58	0.615	0.71	3.31	–

[a] J_{sc}^{IPCE} values were integrated from their IPCE spectra.

LUMO level of **PCA-ZnPc-3** was determined as −0.57 vs. NHE, which is higher than the conduction band of TiO$_2$ (−0.5 V vs. NHE), ensuring the sufficient electron injection (Jia et al., 2016).

3.3. Photovoltaic properties

The photocurrent density–voltage (*J–V*) characteristics of the DSSCs based on **PCA-ZnPc-3** with and without chenodeoxycholic acid (CDCA) as the coadsorbent and the related photovoltaic characteristics i.e., short circuit current density (J_{sc}), open circuit voltage (V_{oc}), fill factor (FF) and power conversion efficiency (PCE) were shown in Fig. 2a and Table 2. The device with **PCA-ZnPc-3** exhibited a higher PCE of 1.97% as compared to the devices based on our previous dyes **PCA-ZnPc-1** (PCE = 1.29%) and **PCA-ZnPc-2** (PCE = 1.67%). Similarly, for the cell based on **PCA-ZnPc-3**, compared with previous dyes, J_{sc} increased from 3.18 and 3.98 mA cm^{-2} to 4.64 mA cm^{-2}, while V_{oc} increased from 0.605 and 0.601 V to 0.624 V, respectively. Although the dye loading of **PCA-ZnPc-1** has higher than those of the others, the lower J_{sc} of **PCA-ZnPc-1** can be ascribed to the dye aggregation which quenches the excitons and inhibits electron injection (Chaurasia et al., 2017). In the presence of CDCA, the cell with **PCA-ZnPc-3** exhibits a higher PCE of 2.04% with a J_{sc} of 4.70 mA cm^{-2} and V_{oc} of 0.630 V. Under the same conditions, the cells with **PCA-ZnPc-1** and **PCA-ZnPc-2** showed inferior photovoltaic performances of 1.74% (J_{sc} = 3.18 mA cm^{-2}, V_{oc} = 0.628 V) and 1.89% (J_{sc} = 4.27 mA cm^{-2}, V_{oc} = 0.611 V). The PCE of the DSSC based on **PCA-ZnPc-3** achieves about 62% of the reference DSSC using **TT1** dye (3.31%). This result is probably attributed to the poor electronic communication due to the non-conjugated oxygen linker adjacent to the anchoring group (Cid et al., 2009). According to the data, the addition of CDCA can improve the PCE for the three dyes. The improvement is explained by the increase of both J_{sc} and V_{oc}. As previously reported (Yıldız et al., 2018), **PCA-ZnPc-1** showed 35% improvement in PCE as compared to that in the absence of CDCA, which may be due to the serious dye aggregation on TiO$_2$ (Tian et al., 2010). In contrast to **PCA-ZnPc-1**, the PCEs for the DSSCs with hexylsulfanyl (**PCA-ZnPc-2**) and 2,6-diphenylphenoxy (**PCA-ZnPc-3**) donor groups improved by only 13% and 4% in the presence of CDCA, indicating that the aggregation may be weak or negligible for these dyes (Tian et al., 2010). Evidently, it can be related to three-dimensional or bulky structure of donor groups in the latter dyes (Jiang et al., 2010). Generally, bulky groups may provide the ordered molecular arrangement and aggregate-free dye layer on the TiO$_2$ surface, resulting in higher J_{sc} (Jiang et al., 2010). Furthermore, these groups may lead to surface blocking effect through steric hindrance, suppressing the electron recombination, favoring higher V_{oc} (Jiang et al., 2010). Comparing the two dyes with bulky donor groups, the dye loading of **PCA-ZnPc-2** (2.76×10^{-8} mol cm^{-2}) is less than that of **PCA-ZnPc-3** (3.12×10^{-8} mol cm^{-2}), probably due to the linear structure of hexylsulfanyl groups in the former dye. The higher dye loading of **PCA-ZnPc-3** can not only improve the light-harvesting ability but also reduce the free volume for penetration of the redox electrolyte to the TiO$_2$, resulting in a higher J_{sc} and V_{oc} (Jia et al., 2019; Lee et al., 2021). As a result, the better photovoltaic performance of **PCA-ZnPc-3** relative to **PCA-ZnPc-2** is probably due to its higher dye loading amount.

Fig. 2b shows the incident photon-to-current conversion efficiencies (IPCE) as a function of the light excitation wavelength for the devices with **PCA-ZnPc-3**. As shown in Table 2, the photocurrent densities calculated by integrating the IPCE values (J_{sc}^{IPCE}) match well with J_{sc} values observed in the *J–V* curves, indicating the accuracy of the results. It can be also seen that the IPCE responses are in the range of 350–750
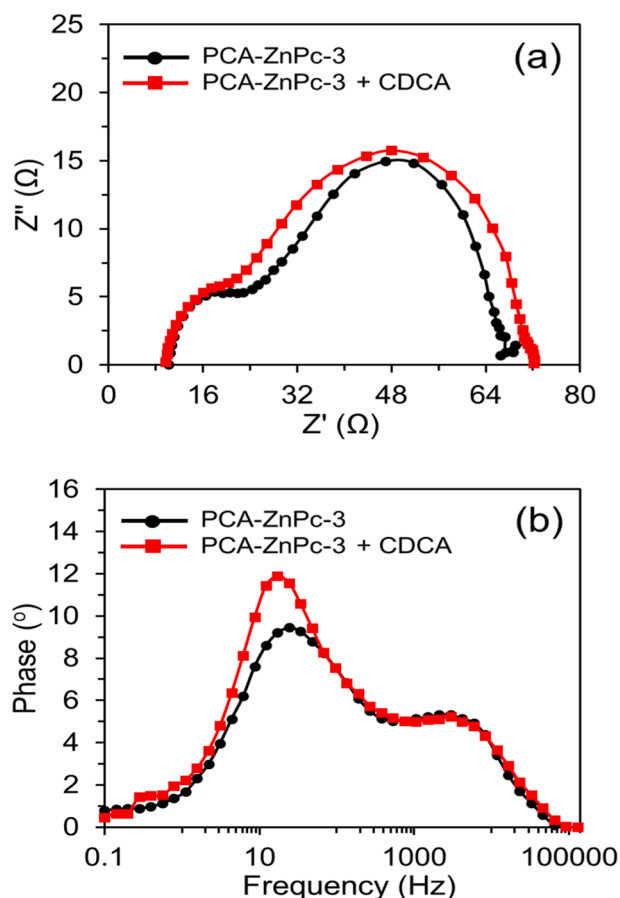
Fig. 3. (a) Nyquist and (b) Bode plots of the DSSCs.

nm, which is in well agreement with the absorption spectrum on TiO_2 surface. The IPCE value of **PCA-ZnPc-3** was enhanced slightly with the addition of coadsorbent as compared to **PCA-ZnPc-1**, suggesting the bulky donor groups in the former can prevent dye aggregation (Arslan et al., 2021; Shi et al., 2012).

Electrochemical impedance spectroscopy (EIS) was employed to confirm the difference of V_{oc} between the DSSCs with and without CDCA in the dark at a forward bias of − 0.60 V. As shown in Fig. 3a, the radius of the larger semicircle at the low frequency region in the Nyquist plots

expresses the charge recombination resistance (R_{rec}) at TiO2/dye/electrolyte interface, which is related with V_{oc} value showed by the DSSC. The R_{rec} for **PCA-ZnPc-3 + CDCA** (46.7 Ω) is slightly higher than that of **PCA-ZnPc-3** (43.2 Ω). Similarly, the electron lifetimes (τ_e), which can be calculated by the peak frequency (f) in the low-frequency region in Bode plots using $\tau_e = 1/2\pi f$, are 7.1 and 8.9 ms for **PCA-ZnPc-3** and **PCA-ZnPc-3 + CDCA** (Fig. 3b). Obviously, both R_{rec} and τ_e are consistent with the sequence of V_{oc} values obtained in *J–V* curves.

The photostability of the DSSC based on **PCA-ZnPc-3** was also examined during 72 h under simulated sunlight. At the end of this period, it was found that the DSSC maintained 89% of its initial PCE.

3.4. Theoretical calculations

All optimizations were carried out by Gaussian 09 in the gas phase in which DFT calculations were utilized by using the B3LYP/6-311G(d,p) basis set (Raghavachari et al., 1980; McLean and Chandler, 1980; Lee et al., 1988, Becke, 1993; Frisch et al., 2009, Farley et al., 2016). Geometrically optimized structure of **PCA-ZnPc-3** uncovered that the phthalocyanine core is planar and perpendicular to the pyrazole unit. All diphenylphenoxy units are vertical to the phthalocyanine (Fig. 4).

Electron transfer between two important orbitals, HOMO and LUMO, is considered to understand solar cells' capacity in detail. Theoretical calculation and plotting of frontier molecular orbitals were, therefore, calculated using the same hybrid method. HOMO and LUMO of **PCA-ZnPc-3** were localized on the phthalocyanine skeleton with small differences (Fig. 5). Although HOMO consists of all ZnPc frames, LUMO was restricted on the ZnPc unit except that two phenyl rings of ZnPc, perpendicular to the phenoxy-pyrazole group, did not give extreme contribution to LUMO. There are three phenoxy units that carry two identical phenyl rings attached to phthalocyanine. However, neither phenoxy-pyrazole-carboxylic acid unit nor phenoxy units did have a contribution to HOMO or LUMO orbitals. In our previous studies in which the pyrazole ring was used, we have seen almost the same theoretical band gap between 2.17 and 2.14 eV and the corresponding power conversion efficiency between 1.74 and 1.89%. These results showed that attached groups on the aromatic core, such as *tert*-butyl and hexylsulfanyl, did not change the solar cell's electronic capacity. However, in this study, we have advanced the yield of the cell up to 2.04%, although the band gap calculated as 2.14 eV, did not change (Fig. 5). The increase of the cell yield might be due to bulky diphenylphenoxy units, which regulate the aggregation of molecules (Fig. 4). This was also proved with increasing V_{oc} value, which was found as 0.630 V in this
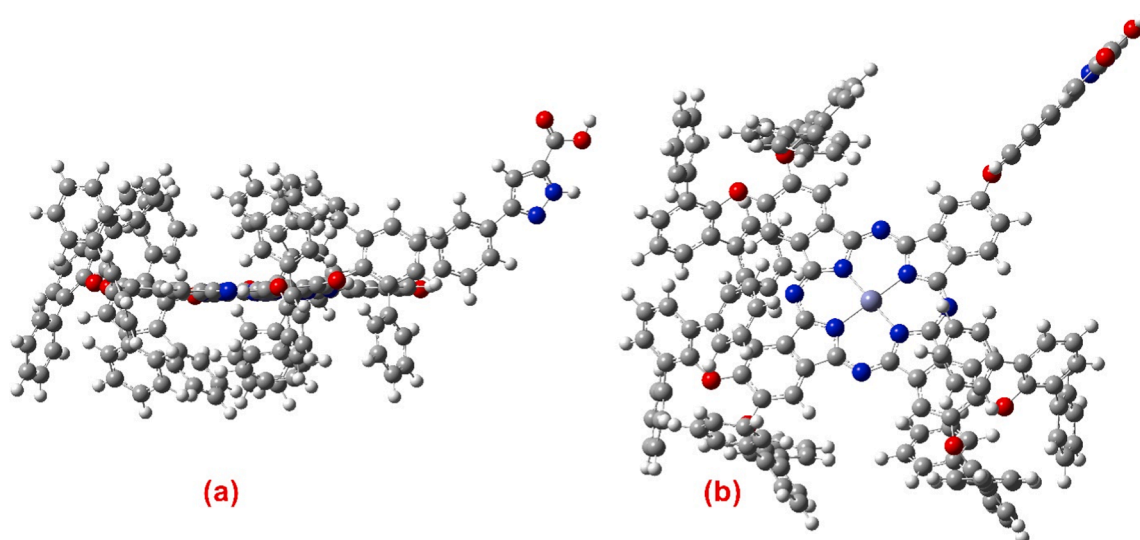

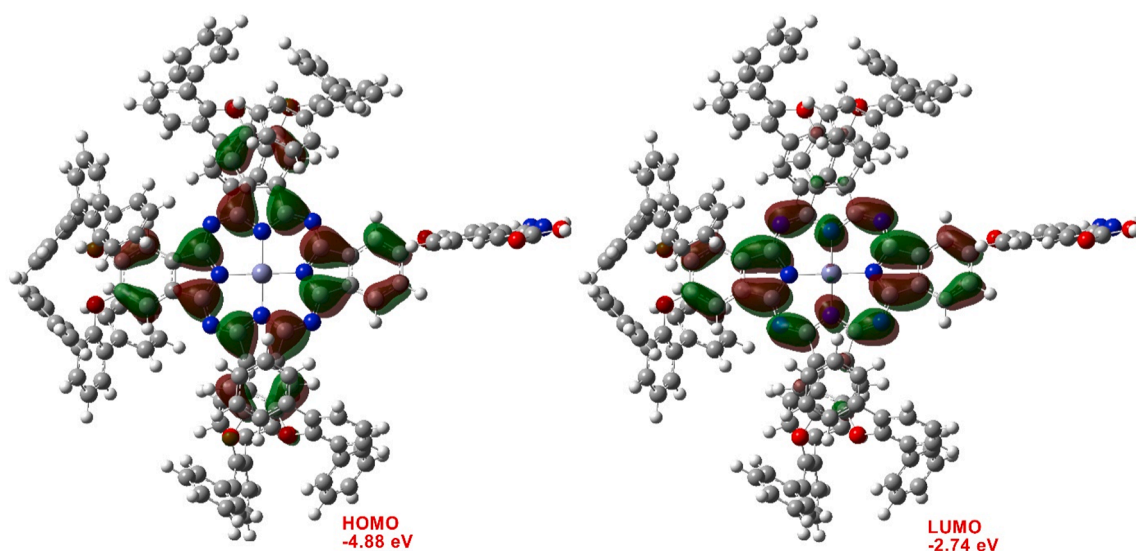**Fig. 4.** Two different visions for **PCA-ZnPc-3**. (a) In front view; (b) side view.

Fig. 5. HOMO and LUMO orbitals for **PCA-ZnPc-3**.

study.

4. Conclusions

In this study, a push-pull zinc phthalocyanine dye (**PCA-ZnPc-3**) having 2,6-diphenylphenoxy donor groups and pyrazole-3-carboxylic acid anchoring group was synthesized for DSSCs. Both electronic absorption and electrochemical measurements have verified that the synthesized dye may be used as a sensitizer. It performed a higher power conversion efficiency of 2.04% (J_{sc} = 4.70 mA cm^{-2}, V_{oc} = 0.63 V, FF = 0.69) with respect to **PCA-ZnPc-1** (1.74%) and **PCA-ZnPc-2** (1.89%). The better photovoltaic performance of **PCA-ZnPc-3** may be attributed to its non-aggregation characteristics. These results confirmed that 2,6-diphenylphenoxy moiety is a promising donor group to improve photovoltaic performance of zinc phthalocyanine-based DSSCs.

Declaration of Competing Interest

The authors declare that they have no known competing financial interests or personal relationships that could have appeared to influence the work reported in this paper.

Acknowledgements

Appendix A. Supplementary material

Supplementary data to this article can be found online at https://doi.org/10.1016/j.solener.2021.08.033.

References

Arslan, B.S., Arkan, B., Gezgin, M., Derin, Y., Avcı, D., Tutar, A., Nebioğlu, M., Şişman, İ., 2021. The improvement of photovoltaic performance of quinoline-based dye-sensitized solar cells by modification of the auxiliary acceptors. J. Photochem. Photobiol. A Chem. 404, 1–10. https://doi.org/10.1016/j.jphotochem.2020.112936.

Becke, A.D., 1993. Density-Functional thermochemistry. III. The role of exact exchange. J. Chem. Phys. 98 (7), 5648–5652. https://doi.org/10.1063/1.464913.

Chaurasia, S., Li, C.-T., Desta, M.B., Ni, J.-S., Lin, J.T., 2017. Benzimidazole/pyridoimidazole-based organic sensitizers for high-performance dye-sensitized solar

cells. Chem.-An Asian J. 12 (9), 996–1004. https://doi.org/10.1002/asia.v12.910.1002/asia.201700039.

Cid, J.-J., García-Iglesias, M., Yum, J.-H., Forneli, A., Albero, J., Martínez-Ferrero, E., Vázquez, P., Grätzel, M., Nazeeruddin, M., Palomares, E., Torres, T., 2009. Structure-function relationships in unsymmetrical zinc phthalocyanines for dye-sensitized solar cells. Chem. - A Eur. J. 15 (20), 5130–5137. https://doi.org/10.1002/chem.v15:2010.1002/chem.200801778.

Cid, J.-J., Yum, J.-H., Jang, S.-R., Nazeeruddin, M., Martínez-Ferrero, E., Palomares, E., Ko, J., Grätzel, M., Torres, T., 2007. Molecular cosensitization for efficient panchromatic dye-sensitized solar cells. Angew. Chemie-Int. Ed. 46 (44), 8358–8362. https://doi.org/10.1002/(ISSN)1521-377310.1002/anie.v46:4410.1002/anie.200703106.

Dinçer, H.A., Şener, M.K., Koca, A., Gül, A., Koçak, M.B., 2008. Synthesis, electrochemistry and in situ spectroelectrochemistry of soluble lead phthalocyanines. Electrochim. Acta 53 (9), 3459–3467. https://doi.org/10.1016/j.electacta.2007.11.060.

Farley, C., Bhupathiraju, N.V.S.D.K., John, B.K., Drain, C.M., 2016. Tuning the structure and photophysics of a fluorous phthalocyanine platform. J. Phys. Chem. A 120 (38), 7451–7464. https://doi.org/10.1021/acs.jpca.6b0702410.1021/acs.jpca.6b07024.s001.

Frisch, M.J., Trucks, G.W., Schlegel, H.B., Scuseria, G.E., Robb, M.A., Cheeseman, J.R., Scalmani, G., Barone, V., Mennucci, B., Petersson, G.A., Nakatsuji, H., Caricato, M., Li, X., Hratchian, H.P., Izmaylov, A.F., Bloino, J., Zheng, G., Sonnenberg, J.L., Hada, M., Ehara, M., Toyota, K., Fukuda, R., Hasegawa, J., Ishida, M., Nakajima, T., Honda, Y., Kitao, O., Nakai, H., Vreven, T., Montgomery Jr., J.A., Peralta, J.E., Ogliaro, F., Bearpark, M., Heyd, J.J., Brothers, E., Kudin, K.N., Staroverov, V.N., Kobayashi, R., Normand, J., Raghavachari, K., Rendell, A., Burant, J.C., Iyengar, S.S., Tomasi, J., Cossi, M., Rega, N., Millam, J.M., Klene, M., Knox, J.E., Cross, J.B., Bakken, V., Adamo, C., Jaramillo, J., Gomperts, R., Stratmann, R.E., Yazyev, O., Austin, A.J., Cammi, R., Pomelli, C., Ochterski, J.W., Martin, R.L., Morokuma, K., Zakrzewski, V. G., Voth, G.A., Salvador, P., Dannenberg, J.J., Dapprich, S., Daniels, A.D., Farkas, Ö., Foresman, J.B., Ortiz, J. V, Cioslowski, J., Fox, D.J., 2009. Gaussian 09, Revision D.01, Gaussian Inc. https://doi.org/10.1159/000348293.

Jia, H.-L., Peng, Z.-J., Gong, B.-Q., Huang, C.-Y., Guan, M.-Y., 2019. New 2D-π-2A organic dyes with bipyridine anchoring groups for DSSCs. New J. Chem. 43 (15), 5820–5825. https://doi.org/10.1039/C9NJ00087A.

Jia, H.-L., Zhang, M.-D., Yan, W., Ju, X.-H., Zheng, H.-G., 2016. Effects of structural optimization on the performance of dye-sensitized solar cells: Spirobifluorene as a promising building block to enhance v oc. J. Mater. Chem. A 4 (30), 11782–11788. https://doi.org/10.1039/C6TA03740B.

Jiang, X., Marinado, T., Gabrielsson, E., Hagberg, D.P., Sun, L., Hagfeldt, A., 2010. Structural modification of organic dyes for efficient coadsorbent-free dye-sensitized solar cells. J. Phys. Chem. C 114 (6), 2799–2805. https://doi.org/10.1021/jp908552t.

Lee, C., Yang, W., Parr, R.G., 1988. Development of the Colle-Salvetti correlation-energy formula into a functional of the electron density. Phys. Rev. B 37 (2), 785–789. https://doi.org/10.1103/PhysRevB.37.785.

Lee, M.W., Kim, J.Y., Lee, H.G., Cha, H.G., Lee, D.H., Ko, M.J., 2021. Effects of structure and electronic properties of D-π-A organic dyes on photovoltaic performance of dye-sensitized solar cells. J. Energy Chem. 54, 208–216. https://doi.org/10.1016/j.jechem.2020.05.060.

Matsuzaki, H., Murakami, T.N., Masaki, N., Furube, A., Kimura, M., Mori, S., 2014. Dye aggregation effect on interfacial electron-transfer dynamics in zinc phthalocyanine-sensitized solar cells. J. Phys. Chem. C 118 (31), 17205–17212. https://doi.org/10.1021/jp500798c.

McLean, A.D., Chandler, G.S., 1980. Contracted Gaussian-basis sets for molecular calculations. 1. 2nd row atoms, Z=11-18. J. Chem. Phys. 72, 5639–5648. https://doi.org/10.1063/1.438980.

Mori, S., Nagata, M., Nakahata, Y., Yasuta, K., Goto, R., Kimura, M., Taya, M., 2010. Enhancement of incident photon-to-current conversion efficiency for phthalocyanine-sensitized solar cells by 3D molecular structuralization. J. Am. Chem. Soc. 132 (12), 4054–4055. https://doi.org/10.1021/ja9109677.

Raghavachari, K., Binkley, J.S., Seeger, R., Pople, J.A., 1980. Self-consistent molecular orbital methods. 20. Basis set for correlated wave-functions. J. Chem. Phys. 72, 650–654. https://doi.org/10.1063/1.438955.

Ragoussi, M.-E., Cid, J.-J., Yum, J.-H., delaTorre, G., DiCenso, D., Grätzel, M., Nazeeruddin, M.K., Torres, T., 2012. Carboxyethynyl anchoring ligands: A means to improving the efficiency of phthalocyanine-sensitized solar cells. Angew. Chem. – Int. Ed. 51 (18), 4375–4378. https://doi.org/10.1002/anie.201108963.

Ragoussi, M.-E., Ince, M., Torres, T., 2013. Recent advances in phthalocyanine-based sensitizers for dye-sensitized solar cells. European J. Org. Chem. 2013 (29), 6475–6489. https://doi.org/10.1002/ejoc.v2013.2910.1002/ejoc.201301009.

Reddy, P., Giribabu, L., Lyness, C., Snaith, H., Vijaykumar, C., Chandrasekharam, M., Lakshmikantam, M., Yum, J.-H., Kalyanasundaram, K., Grätzel, M., Nazeeruddin, M., 2007. Efficient sensitization of nanocrystalline TiO2 films by a near-IR-absorbing unsymmetrical zinc phthalocyanine. Angew. Chem. - Int. Ed. 46 (3), 373–376. https://doi.org/10.1002/(ISSN)1521-377310.1002/anie.v46:310.1002/anie.200603098.

Saçmacı, Ş., Kartal, Ş., 2008. Selective extraction, separation and speciation of iron in different samples using 4-acetyl-5-methyl-1-phenyl-1H-pyrazole-3-carboxylic acid. Anal. Chim. Acta 623 (1), 46–52. https://doi.org/10.1016/j.aca.2008.05.073.

Sánchez-Vergara, M.E., Gómez-Gómez, M., Hamui, L., Álvarez-Bada, J.R., Jiménez-Sandoval, O., 2021. Optoelectronic behaviour of zinc phthalocyanines doped with anthraquinone derivatives and their potential use in flexible devices. Mater. Technol. 36 (4), 250–259. https://doi.org/10.1080/10667857.2020.1747807.

Shi, J., Huang, J., Tang, R., Chai, Z., Hua, J., Qin, J., Li, Q., Li, Z., 2012. Efficient metal-free organic sensitizers containing tetraphenylethylene moieties in the donor part for dye-sensitized solar cells. European J. Org. Chem. 2012 (27), 5248–5255. https://doi.org/10.1002/ejoc.201200530.

Shi, W., Peng, B., Lin, L., Li, R., Zhang, J., Peng, T., 2015. Effect of carboxyl anchoring groups in asymmetric zinc phthalocyanine with large steric hindrance on the dye-sensitized solar cell performance. Mater. Chem. Phys. 163, 348–354. https://doi.org/10.1016/j.matchemphys.2015.07.049.

Şener, A., Akbaş, E., Şener, M.K., 2004. Synthesis and some reactions of 4-benzoyl-5-phenyl-1-pyridin-2-yl-1H- pyrazole-3-carboxylic acid. Turkish J. Chem. 28, 271–277.

Tian, H., Yang, X., Cong, J., Chen, R., Teng, C., Liu, J., Hao, Y., Wang, L., Sun, L., 2010. Effect of different electron donating groups on the performance of dye-sensitized solar cells. Dye. Pigment. 84 (1), 62–68. https://doi.org/10.1016/j.dyepig.2009.06.014.

Urbani, M., Ragoussi, M.E., Nazeeruddin, M.K., Torres, T., 2019. Phthalocyanines for dye-sensitized solar cells. Coord. Chem. Rev. 381, 1–64. https://doi.org/10.1016/j.ccr.2018.10.007.

Yıldız, B., Güzel, E., Akyüz, D., Arslan, B.S., Koca, A., Şener, M.K., 2019. Unsymmetrically pyrazole-3-carboxylic acid substituted phthalocyanine-based photoanodes for use in water splitting photoelectrochemical and dye-sensitized solar cells. Sol. Energy 191, 654–662. https://doi.org/10.1016/j.solener.2019.09.043.

Yıldız, B., Güzel, E., Menges, N., Şişman, İ., Şener, M.K., 2018. Pyrazole-3-carboxylic acid as a new anchoring group for phthalocyanine-sensitized solar cells. Sol. Energy 174, 527–536. https://doi.org/10.1016/j.solener.2018.09.039.

Yu, L., Zhou, X., Yin, Y., Liu, Y., Li, R., Peng, T., 2012. Highly asymmetric tribenzonaphtho-condensed porphyrazinatozinc complex: An efficient near-infrared sensitizer for dye-sensitized solar cells. Chempluschem 77 (11), 1022–1027. https://doi.org/10.1002/cplu.v77.1110.1002/cplu.201200219.